CHAPTER III
INVESTIGATING PROTON TRANSFERRING ROUTE IN HETEROAROMATIC COMPOUND PART I: A TRIAL TO DEVELOP DI- AND TRI-FUNCTIONAL BENZIMIDAZOLE MODEL COMPOUNDS AND THEIR HYDROGEN BOND NETWORK

3.1 Abstract

Di- and trifunctional benzimidazole molecules have been synthesized as the model compounds to identify their molecular packing structure and hydrogen bond network, which possibly involves in proton transfer system belonging to its heteroaromatic functional groups. By carrying out the reaction between acid chloride and diamine, the desired benzimidazole compounds were obtained (yield over 60%). The comparison studies between the compounds and benzimidazole reveal that the model compounds show well-packing structure with intermolecular hydrogen bond similar to those observed in benzimidazole. The presence of solvent with **2** leads to the unique intermolecular hydrogen bonds between one molecule of **2** and six molecules of solvent, i.e., 2-propanol, resulting in the solvent-assisted intramolecular hydrogen bond network among benzimidazole functional groups. Studies of the effect of temperature on the packing structure and hydrogen bond in the compound indicate that the model compounds have stronger intermolecular interaction and higher thermal stability of the molecular packing structure. The simplified structure with regular arrangement of heterocycles leads us to further develop an effective proton transfer mechanism in proton exchange membrane.

Keywords: Proton Conductivity, Proton Transfer, Fuel Cell, Polymer Electrolyte Membrane Fuel Cell, Benzimidazole

3.2 Introduction

Proton transfer in hydrated perfluorosulphonic acid polymer, which is based on the hydrogen bond between water molecules (hydranium ion) and sulphonate group throughout the hydrophilic cluster channel, is recognized as a key mechanism in polymer electrolyte membrane fuel cell (PEMFC).[1-3] As the path way of hydranium ion is random,[4-5] the enhancement of proton conductivity has to be relied on the specific conditions such as acid treatment, humidity, thermal acceleration of proton movement etc. The operating condition at intermediate temperature (120-160°C) is another requirement if we consider the activation of catalyst on electrodes.[6,8-10] Unfortunately, the consequent loss of water molecules in the membrane due to evaporation above 80°C and cost of the commercially available membrane, Nafion®, limit the usage of PEMFC.[3,11] Recently, an alternative system of polymer electrolyte membrane has been introduced based on the mechanism of proton transferring in water-free condition. In this system, the function of heterocyclic compounds, especially imidazole, benzimidazole, and pyrazole, was proposed to play a role as the proton carrier in dry system even at high temperature via a mechanism involving proton transfer- and reorientation process.[12-15] Considering this proton transfer mechanism, the regularity on molecular arrangement of the compound is essential. However, most studies on the materials are about the heterocyclic moieties incorporated in the main chain,[12,16-17] side chain [18-20] or mixed as the filler in polymer matrix.[21-23] The effective proton transferring route is still needed to be clarified in details to overcome the low mobility of the heteroaromatic groups and the lack of molecular arrangement of the proton carrier parts.

In order to obtain an effective proton transfer property, the proton transfer mechanism has to be favored by developing a molecularly-aligned system of heterocyclic compounds, which make the proton hopping occur easily. However, this kind of work is rarely reported. One possibility is to build up a well-defined proton transferring route based on the specific molecular arrangement. On this viewpoint, the present work proposes the molecular design and synthesis of *ethylene-1,2-di-2-benzimidazole*, **1**, (difunctional benzimidazole) and *benzene-1,3,5-tri-2-*

benzimidazole, **2**, (trifunctional benzimidazole) to be the model compounds inducing the formation of molecular packing structures which further act as effective proton transferring path. Compound **1** is attractive in terms of the more number of proton carriers as compared with a single benzimidazole, the symmetrical structure and the possibly high thermal stability, whereas compound **2** shows further advantages of the planar shape which might enhance the π-π stacking conformation, also the more number of benzimidazole units and higher thermal stability. The works also extend to an investigation about how the hydrogen bond networks formed in the materials including the change in packing structures and hydrogen bond under the effects of solvent molecules and temperature as compared with single benzimidazole compound. We will discuss these points on the basis of the simultaneous measurement of wide-angle X-ray diffraction (WAXD) and differential scanning calorimetric (DSC) thermogram, temperature dependent Fourier transform infrared (FTIR) spectroscopy, and the single crystal X-ray structure analysis.

3.3 Experimental

3.3.1 Materials

Benzimidazole, 1,3,5-benzenetricarbonyltrichloride and 1,2-phenylenediamine were purchased from Aldrich, Germany. Succinyl chloride was bought from Fluka, Switzerland. All chemicals and solvents were analytical grade and were used without further purification.

3.3.2 Synthesis of **1**

Compound **1** was synthesized as shown in Scheme 3.1. Succinyl chloride (1.30 g, 7.97×10^{-3} mol) in xylene (150 ml) was added dropwisely into a vigorously stirred solution of 1,2-phenylenediamine (2.66 g, 2.45×10^{-2} mol) in xylene (50 ml) at 80°C under nitrogen atmosphere. The reaction was proceeded for 24 hours yielding the dark green precipitate. The precipitate was collected and dissolved in methanol prior reprecipitated by adding 1.0 M NaOH solution. The purple precipitate was obtained as a product.

Characterization: FT-IR (cm^{-1}): 3450 (weak, N-H stretching); 3200-2500 (strong, hydrogen bonded N-H stretching); 1452 and 1436 (strong, skeleton vibration of benzimidazole ring); 746 (strong, aromatic C-H bending). ^1H NMR (DMSO-d_6): δ 7.50 (4H, d, Ar-H); 7.10 (4H, s, Ar-H); 3.20 (4H, s, CH_2). Mass spectrometry (m/z): 263.13. FW of $C_{16}H_{14}N_4$: 262. Elemental analysis (%) Found: C 71.99. H 5.70. N 20.49. Calcd. for $C_{27}H_{18}N_6$: C 73.28. H 5.34. N 21.37.

3.3.3 Synthesis of **2**

The steps of reaction are summarized in Scheme 3.2. 1,3,5-Benzenetricarbonyltrichloride (0.2310 g, 8.53×10^{-4} mol) in xylene (150 ml) was added dropwisely into a vigorously stirred solution of 1,2-phenylenediamine (0.3820 g, 3.51×10^{-3} mol) in xylene (50 ml) at 70°C under nitrogen atmosphere. The red brownish precipitates were obtained after overnight. The precipitates were washed a few times with xylene before neutralizing in methanol with 1.0 M NaOH solution to obtain green yellow solution. The solvent was changed from methanol to ethylene glycol and the solution was refluxed at 150°C under vacuum for 24 h to obtain yellow precipitates. The product was washed several times with distilled water and recrystallized in methanol before kept drying in vacuum to obtain *benzene-1,3,5-tri-2-benzimidazole*, **2.** Single crystals necessary for X-ray structure analysis were prepared by further recrystallization in 2-propanol.

Characterization: FT-IR (cm^{-1}): 3500-2800 (strong, hydrogen bonded N-H and O-H stretching); 1436 (strong, skeleton vibration of benzimidazole ring); 742 (strong, aromatic C-H bending). ^1H NMR (CD_3OD): δ 8.76 (3H, s, Ar-H (benzene)); 7.62 (6H, br, Ar-H (benzimidazole)); 7.24 -7.27 (6H, dd, Ar-H (benzimidazole)).

Sublimation of **2** was performed at 340 °C under reduced pressure. Characterization: FT-IR (cm^{-1}): 3430 (weak, N-H stretching); 3000-2200 (strong, hydrogen bonded N-H stretching); 1444 (strong, skeleton vibration of benzimidazole ring); 743 (strong, aromatic C-H bending). Mass spectrometry (m/z): 427.16. FW of $C_{27}H_{18}N_6$: 426. Elemental analysis (%) Found: C 73.37. H 4.91. N 18.55. Calcd. For $C_{27}H_{18}N_6$: C 76.06. H 4.23. N 19.72.

3.3.4 Instruments and Equipments

FT-IR spectra were recorded on a Thermo Nicolet Nexus 670 Fourier transform infrared spectrophotometer with 32 scans at a resolution of 2 cm^{-1} in a frequency range of 4000-400 cm^{-1}, using a deuterated triglycinesulfate detector (DTGS). Temperature dependent FTIR spectroscopy was performed with the temperature-controlled sample holder developed in our laboratory. Proton nuclear magnetic resonance (^1H NMR) spectra were collected by a Varian Mercury-400BB spectrometer using tetramethylsilane as an internal standard. DMSO-d_6 and CD_3OD were used as solvents for compound **1** and compound **2**, respectively. Mass spectra were measured with a Bruker micrOTOF mass spectrometer (MS) in positive ion mode. Compound **1** was ionized by electrospray ionization (ESI), whereas compound **2** was ionized by atmospheric pressure chemical ionization (APCI) interface operated at 250 °C under electrical field strength of 4 kV. Thermal analyses were performed with a TA Instrument Q-1000 DSC analyzer scanning from 25 to 500 °C at a heating/cooling rate of 10°C/min under nitrogen atmosphere. Elemental analyses were done by a Bruker 2000 series III CHNO/S analyzer. Simultaneous wide angle X-ray diffraction (WAXD) measurement and DSC analysis were done by using a Rigaku X-ray diffractomer/RINT-TTR III Thermo plus DSC analyzer in the temperature range from 25 to 150 °C at a heating/cooling rate of 3°C/min under nitrogen atmosphere. X-ray single crystal structure analysis was carried out by a Rigaku R-AXIS RAPID-II diffractometer with graphite-monochromated Mo Kα radiation at 296 K. The crystal was kept in capillary filled with 2-propanol. The structure was solved by direct methods (SIR92) and refined by the full matrix least-square procedures on $|F|^2$ (F: structure factor). All non-hydrogen atoms were refined for an anisotropic thermal parameter as well as the fractional coordinates. All the analyses were performed using the "Crystal Structure" software package.

3.4 Results and Discussion

3.4.1 Synthesis of Difunctional Benzimidazole Compound, **1**

Persson *et al.*[7] reported a single step reaction to obtain benzimidazole compound from poly(ethylene glycol) bis(carboxymethyl) ether and 1,2-phenylenediamine. However, after several attempts to prepare **1** from the reaction between succinic acid and phenylenediamine using the similar conditions, we found that the expected difunctional benzimidazole derivative is difficult to be obtained from the reaction of dicarboxylic acid with diamine. Therefore, we changed from dicarboxylic acid to diacid chloride, i.e., succinyl chloride, which has stronger reactivity to diamine than that of carboxylic acid. The reaction took place at 80 °C under nitrogen atmosphere for 24 hours as shown in Scheme 3.1. The excess amount of phenylenediamine together with the dilute concentration and slow addition of succinyl chloride were done to suppress the polymerization reaction between the two reagents. After the reaction finished, purification was done by dissolve the crude product in methanol before adding NaOH into the solution to reprecipitate the final product. The difunctional benzimidazole, **2**, was obtained as purple powder. This one-pot synthesis was found to be an easy and efficient condition to prepare **1** with the yield of 63.6%.

Scheme 3.1 Synthesis of ethylene-1,2-di-2-benzimidazole, **1**.

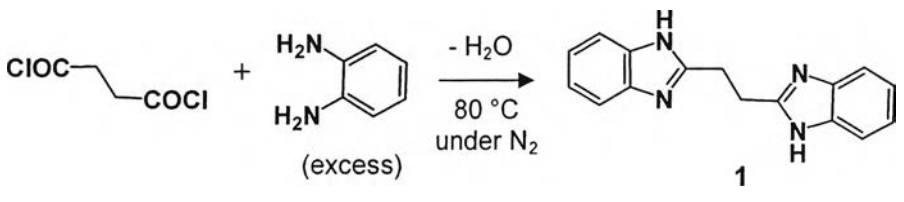

The success of preparation of **1** was confirmed by FTIR, ^{1}H NMR, MS and EA. FTIR spectrum of **1** shows the important peaks of N-H stretching at 3450 cm^{-1}, the characteristic band of hydrogen bonded N-H stretching of benzimidazole unit at 3200-2500 cm^{-1}, skeleton vibration of benzimidazole ring at 1452 and 1436 cm^{-1}, and C-H bending of aromatic at 746 cm^{-1}. ^{1}H NMR spectrum indicates the peaks related to the structure of **1** at 7.50, 7.10 and 3.20 ppm which correspond to the protons at Ar-H position in benzimidazole ring and protons at CH_2

position, respectively. ESI-MS reveals the parent peaks at m/z = 263.13 and 285.43 which represent the molecular weight of **1** with proton and sodium ion, respectively (formula weight of **1** = 262). EA result also supports the accomplishment of the preparation condition with the good agreement of atomic content between the observed one (C 71.99, H 5.70, N 20.49) and the calculated one (Calcd. for $C_{16}H_{14}N_4$: C 73.28, H 5.34, N 21.37). Therefore, all the characterization techniques strongly ensure the successful synthesis of **1**.

3.4.2 Synthesis of Triifunctional Benzimidazole Compound, **2**

In contrast with synthesis of **1**, we found that **2** is difficult to prepare by the single step reaction. Although, the condition was adjusted in many factors, only the amide derivatives were obtained. Thus, we modified the synthesis condition by separating into two steps (i) amidation and (ii) ring closure as shown in Scheme 3.2.

Scheme 3.2 Synthesis of benzene-1,3,5-tri-2-benzimidazole, **2**.

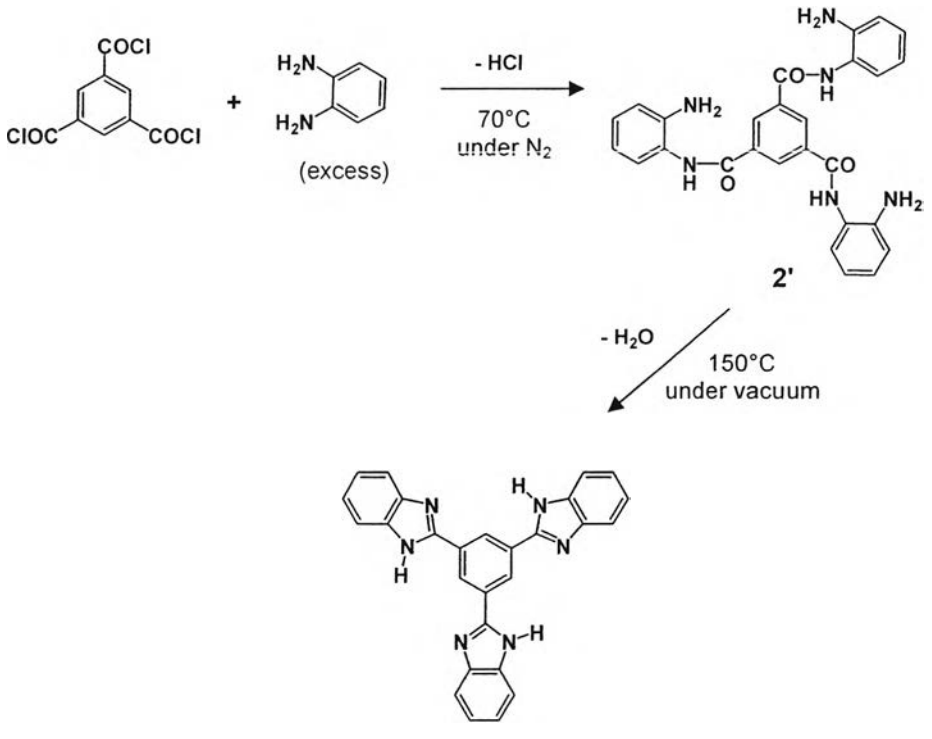

In the first step, after triacid chloride was reacted with the diamine, red brownish precipitates were obtained. The precipitates show the characteristic peaks of amide bond: C=O (amide I) at 1650 cm^{-1} and N-H (amide II) at 1521 cm^{-1} (Figure 3.1(a)). Although, we have not yet strongly confirmed that the trifuntional amide compound, **2'**, was obtained at this step, the neutralization by NaOH was applied to reduce the protonated amines and recover the nucleophilicity of the amino groups for the cyclization in the next step. The amount of NaOH solution is important since an insufficient amount causes a lower extent of cyclization while an excess one induces the cleavage of amide bond via sponification. The equivalent point of neutralization could be easily determined from the change in color of the methanol solution of **2'** from brown to green (pH~6.0). In order to allow the ring closure, **2'** was collected and the second step of reaction was proceeded.

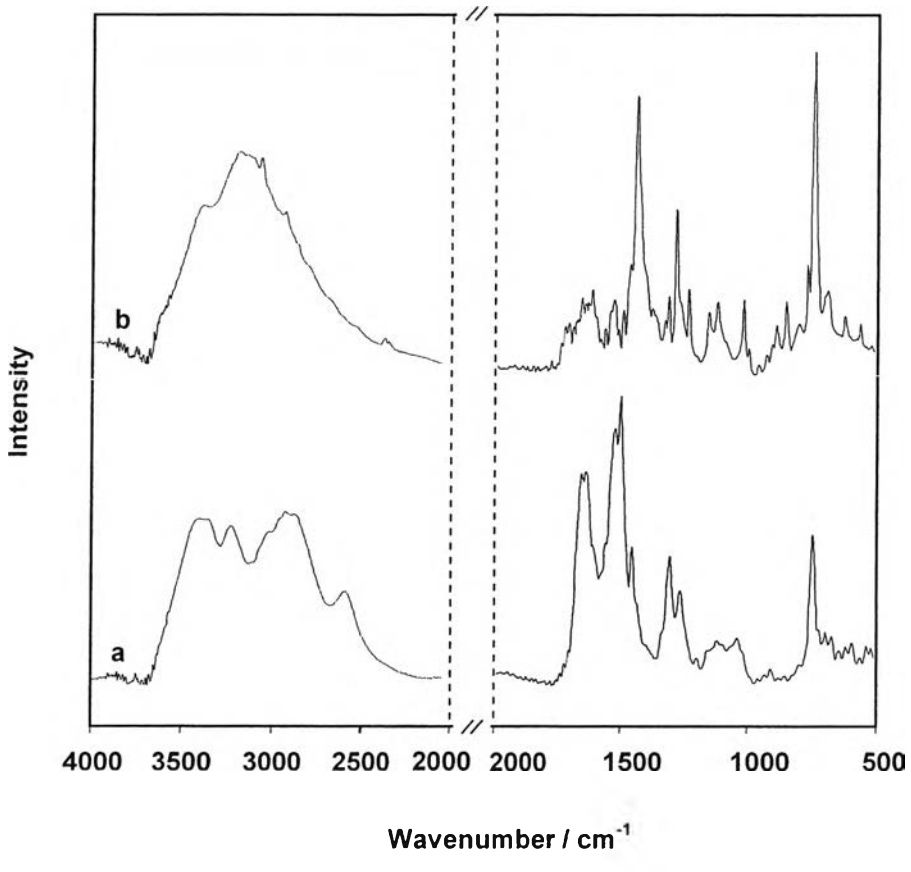

Figure 3.1 FT-IR spectra of **2'** (a), and **2** (b).

In the second step, the ring closure was done in ethylene glycol to obtain the trifunctional benzimidazole compound, **2**, by refluxing at 150°C under reduced pressure. This step also initiates the by-product, i.e. water, removal. The product was precipitated out from the solution and further collected as a yellow precipitate. After purification, the yellow needle crystals of **2** was obtained (yield ~ 69 %). Figure 3.1(b) shows the FTIR spectra confirming the complete benzimidazole ring formation, where the disappearance of the peaks corresponding to amide bonds of intermediate and the presence of a new band at 1436 cm^{-1} implying the skeletal vibration of benzimidazole ring. ^1H NMR and mass spectrum assure us the successful preparation of **2**. For ^1H NMR, the result shows the peaks at 8.76, 7.62, 7.33 ppm representing the protons at center benzene ring, and protons on benzimidazole unit, respectively. The electrospray-TOF MS reveals the parent peak ($M+H^+$) at m/z = 427.16 corresponding with the molecular weight of **2** ($C_{27}H_{18}N_6$: FW = 426). Moreover, EA result also supports the structure of **2** with the observed data of C 73.37%, H 4.91%, N 18.55% (calculated value for $C_{27}H_{18}N_6$: C 76.06%, H 4.23%, N 19.72%). In this way all the results indicate that the synthesis condition is an effective one for three benzimidazole ring cyclization with high selectivity.

3.4.3 Thermal Properties

In order to obtain higher proton conductivity of electrolyte material, higher efficiency of electrochemical reactions on electrodes and better CO tolerant of catalyst, higher temperature of fuel cell system than that of the conventional operating temperature of PEMFC (~ 80 °C) is required. Therefore, thermal properties of the compounds have to be determined. Here, DSC analysis was applied to study the thermal properties of **1** and **2** in the range of 25-500 °C under nitrogen atmosphere. As expected, both **1** and **2** show good thermal stability for temperature over 400 °C. For compound **1**, DSC result reveals degradation temperature at 429 °C without any melting temperature (T_m) being observed. This might be explained by the formation of strong intermolecular hydrogen bond between the molecules as seen in FTIR spectrum (Figure 3.3 (b)). On the other hand, **2** was stable up to 500 °C as shown in Figure 3.2. Considering the DSC thermogram of **2**, the endothermic peak at 119 °C in the first heating cycle represents the evaporation of 2-propanol molecules

incorporated in the crystal structure. The fact that the release of 2-propanol is at 119 °C, which is much higher than its boiling point (82 °C), we conclude that the molecules were tightly bound in **2** and as a result the high energy is required to evaporate out of the crystal lattice. The disappearance of this band in the second heating cycle also confirms that 2-propanol was released completely in the prior cycle. This is an important point to us when we focus on the hydrogen bond formation in the crystal (see *Investigation of hydrogen bond and molecular packing structure in compounds*).

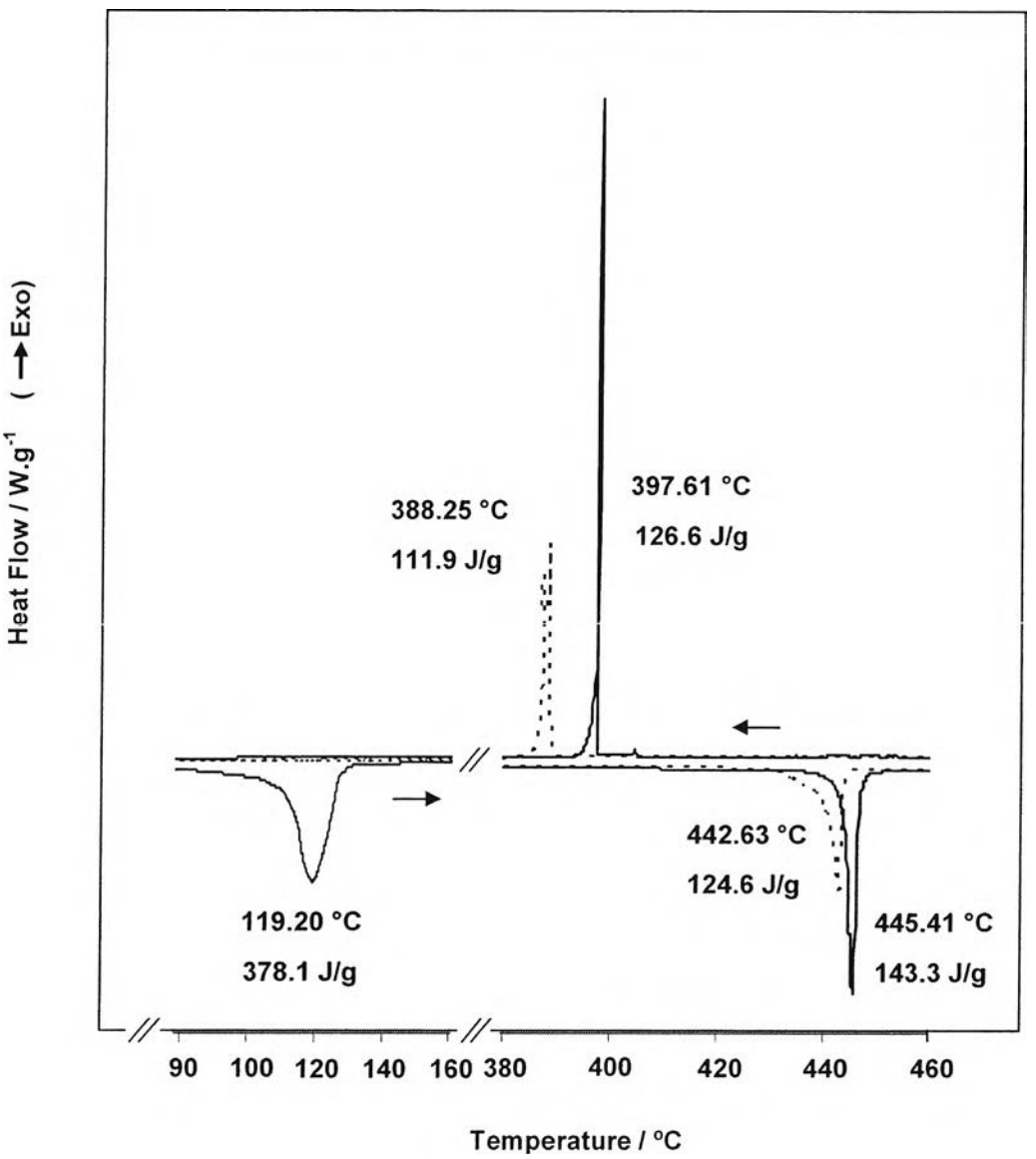

Figure 3.2 DSC thermogram of recrystallized crystal **2**: first heating-cooling cycle (—), and second heating-cooling cycle (---).

For the first heating-cooling cycle, the melting and crystallization peaks were detected at 445 °C and 398 °C, respectively. After performing the second heating-cooling cycle, the melting peak shifts to lower temperature (443 °C) implying the less energy consumed (124.6 J/g) as compared with that of the first cycle (143.3 J/g). We suspect that the packing was more or less affected by the heat. The crystallization peak of the second cycle also shifts to lower temperature (388 °C) with the weaker exothermic peak, implying the effect of the difference in molecular arrangement under different thermal history. The higher temperature and stronger signal of both melting and crystallizing peak in the first cycle than those in the second cycle reflect the higher regularity on molecular arrangement of the crystal obtained from the solution recrystallization than the other one obtained from the crystallization of the melt.

3.4.4 Investigation of Hydrogen Bonds and Molecular Packing Structure in Compounds

Based on the viewpoint of proton hopping mechanism in PEMFC, molecular packing and hydrogen bond network in the compound are important. Here, our compounds were expected to be a model compound favoring the packing of molecules with specific hydrogen bond network between the proton carrying groups, i.e., benzimidazole unit. The more number of benzimidazole unit together with the planar shape of the molecule might induce the molecular packing and result in developing the route of hydrogen bond network, which will be the effective proton transferring path for PEMFC. In order to study the hydrogen bond network formation in compound, investigation of hydrogen bond pattern observed in FTIR spectra is useful information. Figure 3.3 shows the FTIR spectra of **1** (b), crystal **2** obtained from solurion-recrystallization (c), and crystal **2** obtained from sublimation (d) as compared to that of benzimidazole (a). As observed in DSC result, crystal **2** obtained from recrystallization might trap solvent inside the crystal and may affect the FTIR result. Therefore, an attempt to prepare the crystal **2** without solvent was done by subliming **2** at 340 °C *in vacuo*. It is important to note that benzimidazole shows the characteristic bands in the broad region of 3250-2500 cm^{-1}, which can be assigned to

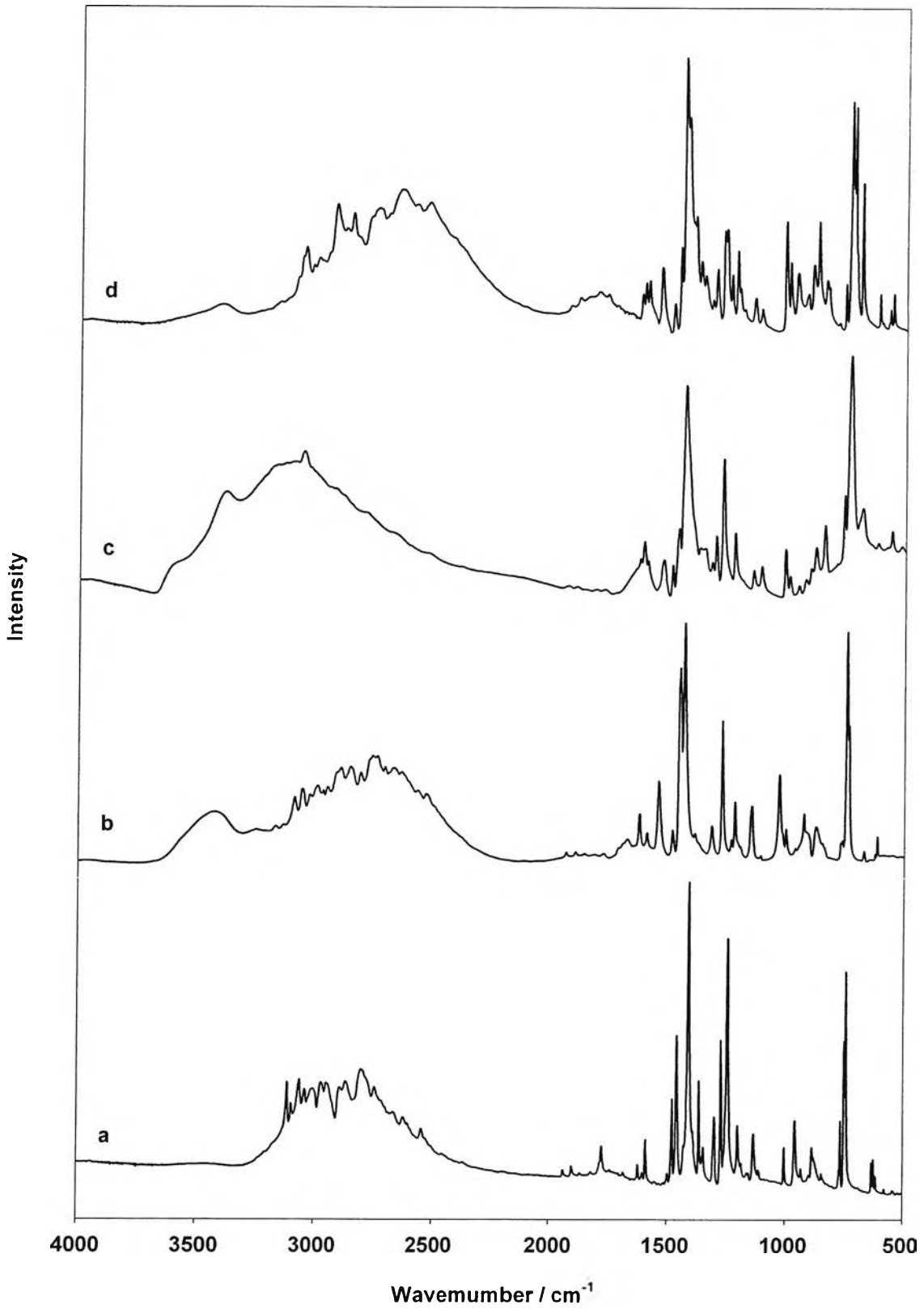

Figure 3.3 FT-IR spectra of crystal benzimidazole (a), **1** (b), crystal **2** obtained from solution-recrystallization (c), and crystal **2** obtained from sublimation (d).

the strong N-H···N intermolecular hydrogen bonds network as illustrated in its crystal structure reported by Vijayan *et. al.*[25] Comparing **1** with benzimidazole, the characteristic peaks representing N-H···N hydrogen bonds are also observed at 3100-2500 cm^{-1}. Therefore, it is reasonable to expect the formation of intermolecular hydrogen bond in **1**. In the case of crystal **2** obtained from recrystallization, the hydrogen bond pattern and position are differed from those of benzimidazole. This might be because of the present of 2-propanol in the crystal which generate the O-H···O or O-H···N type hydrogen bond resulting in the broad peak in bonded O-H stretching region, 3600-2500 cm^{-1}. The explanation is supported by the changes in position and pattern of this characteristic band to 3000-2400 cm^{-1}, which is similar to the case of benzimidazole, after removing the solvent by sublimation (spectrum d). The similar peaks patterns related to hydrogen bond formation of **1**, sublimed crystal **2** and benzimidazole support our expectation of intermolecular hydrogen bond network formation governed by **1** and **2** as it does in case of benzimidazole. Moreover, regarding the fact that the stronger interaction causes the greater shift of the peak to lower region. Therefore, the appearance of the bonded N-H stretching peaks of **1** and **2** in lower frequency region than that of benzimidazole might reflect the stronger hydrogen bond in **1** and **2** than the one presented in benzimidazole.

Molecular packing of the compounds was studied by WAXD analysis. Figure 3.4 shows the WAXD patterns of **1** (a), **2** obtained from recrystallization (b), and **2** obtained from sublimation (c). It should be noted that the transparent single crystal of **2**, which was obtained from recrystallization in 2-propanol, soon turned to opaque when it was left in air atmosphere. This might be due to the evaporation of some solvent trapped inside the crystal. However, when comparing the WAXD patterns of all samples, the results from **1** and sublimed **2** show sharper peaks in all 2θ than that of the recrystallized crystal **2** which has good molecular orientation derived by single crystal. This implies that the molecules of **1** and **2** were in good packing and solvent molecule is not an indispensable factor for good molecular arrangement.

X-ray crystal structure analysis is the useful technique that gives us both molecular packing and hydrogen bond formation of the compound. Here, the

present of strong NH···N intermolecular hydrogen bonds in FTIR spectrum of benzimidazole was further confirmed by analyzing benzimidazole single crystal. The single crystal was prepared by sublimation of benzimidazole at 140 °C *in vacuo*.

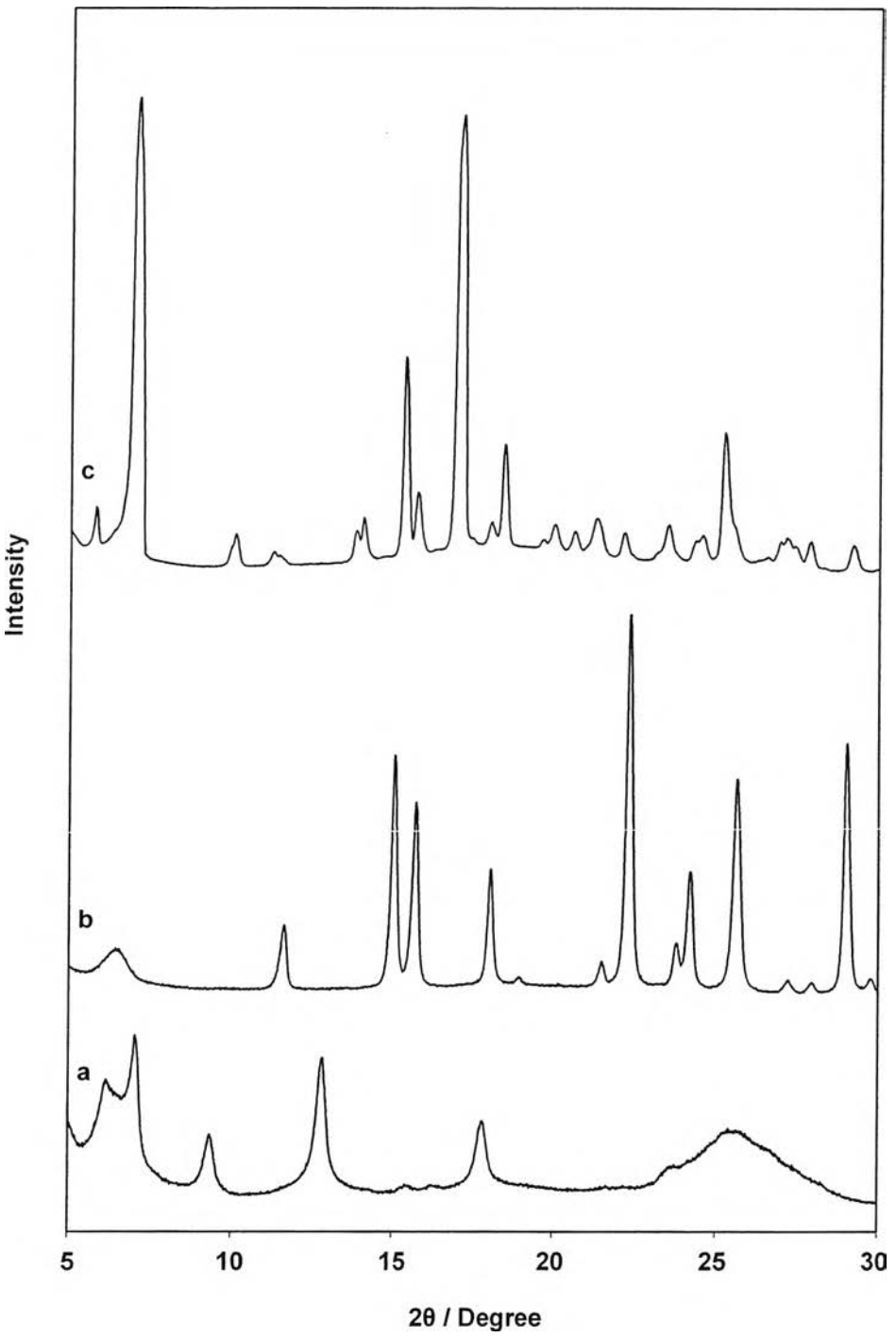

Figure 3.4 WAXD patterns of crystal **2** obtained from solution-recrystallization (a), **1** (b), and crystal **2** obtained from sublimation (c).

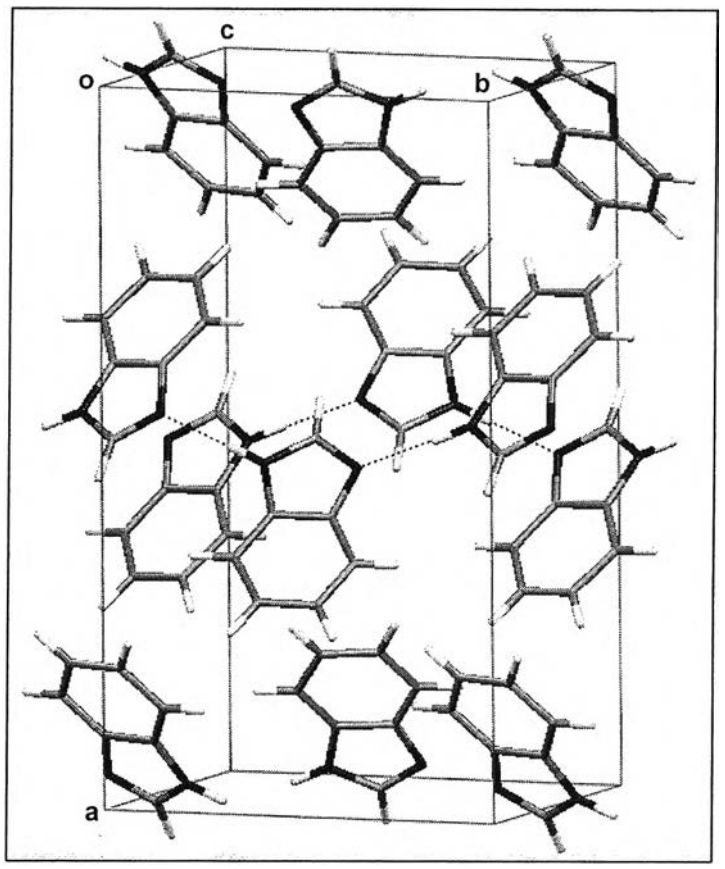

Figure 3.5 Crystal structure of benzimidazole prepared by sublimation. Crystal system: orthorhombic (Pccn); a=16.6754 Å, b=9.7372 Å, c=7.6219 Å; α=β=γ=90°; V=1237.6.

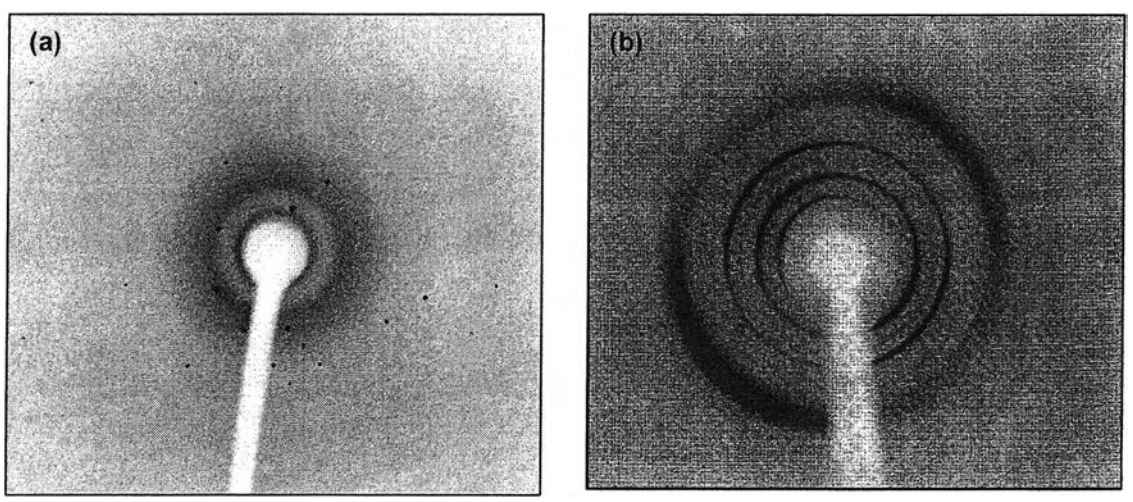

Figure 3.6 2D X-ray diffraction image of crystal **2**: transparent single crystal (a), and turbid crystal (b).

Figure 3.5 shows that the crystal is belonging to orthorhombic crystal system under Pccn with eight molecules in each unit cell. The structure is different from the ones obtained from the solution or melt growth crystals reported previously with $Pna2_1$ and four molecules in the unit cell.[25-26] The result illustrates that the crystal lattice is governed by eight molecules of benzimidazole packed with one dimensional hydrogen bond network along the diazole group. The hydrogen bonds are in a regular network and it is a good reference for our study. For our model compounds, crystals of **1** and sublimed **2** were too small for X-ray single crystal structure analysis. In case of crystal **2** obtained from recrystallization, as mentioned earlier, 2-propanol trapped inside the crystal was not stable and caused the transparent crystal changed to be turbid crystal in air atmosphere. This made the crystal become difficult for analysis. Figure 3.6 shows concrete evidence as seen from the crystalline becoming a mosaic aggregation of small crystals after evaporation of solvent as observed from the 2D XRD. To overcome the problem of solvent instability in the crystal lattice, an attempt to perform X-ray diffraction measurement of the single crystal of **2** immersed in a glass capillary filled with solvent was carried out.

Figure 3.7 illustrates the crystal structure of **2** with 2-propanol. The structure emphasizes the success of our synthesis trifunctional benzimidazole compound. As expected, **2** coexists with 2-propanol in a unit cell: the composition is two molecules of **2** and twelve molecules of 2-propanol. The conformation of **2** is not completely planar: the three benzimidazole rings are slightly out of the plane of the core benzene. The conformational disorder of 2-propanol molecules is considered to occur due to their thermal vibration in the crystal, making the structure analysis be difficult to fix the position of 2-propanol in the crystal lattice as seen from the wide probability of carbon atomic position of 2-propanol in Figure 3.7 (b). This conformational disorder of solvent limited the R value ~13% (without adding H). The existence of hydrogen bonds between the nitrogen atoms of **2** and the oxygen atoms of the nearest 2-propanol molecules were observed with the N···O distance ~2.8 Å [23] (Figure 3.7 (a)). This supports the FTIR result of no N-H···N type hydrogen bond being observed in recrystallized crystal **2**, also the higher evaporating temperature shown in DSC result. These hydrogen bonds may result in the non-

planar conformation of **2** and might help the stabilization of the packing structure of **2** in the crystal lattice.

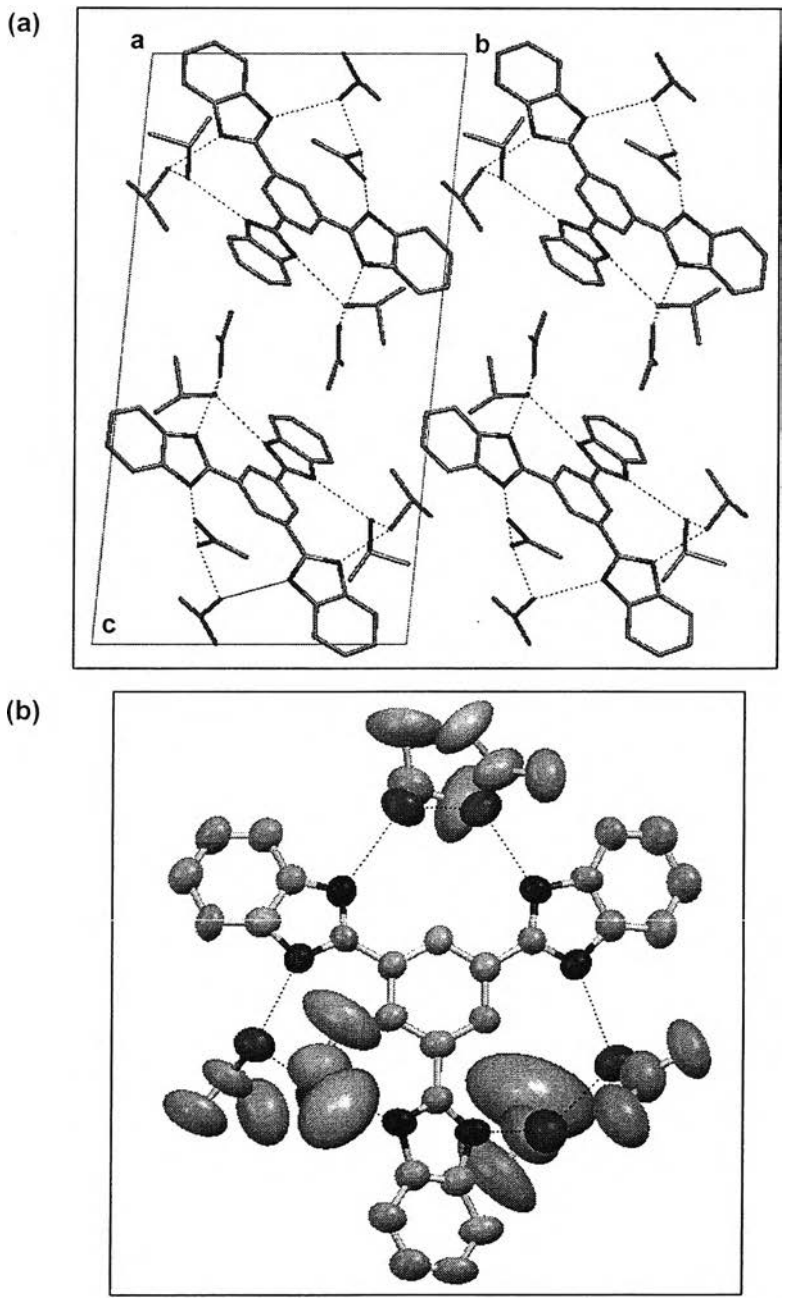

Figure 3.7 Crystal structure of **2** with 2-propanol: overview of hydrogen bond network between **2** and 2-propanol (a), and solvent-assisted intramolecular hydrogen bond network of **2** (b). Crystal system: triclinic (P-1); a=9.081 Å, b=11.991 Å, c=22.376 Å; α=95.134°, β=93.043°, γ=95.515°; V=2394.2.

Another type of hydrogen bonds is also extracted between the solvent molecules in the adjacent position. This leads to a unique characteristic of intermolecular hydrogen bond network between one molecule of **2** and six molecules of 2-propanol resulting in the solvent-assisted intramolecular hydrogen bond network among benzimidazole functional groups in **2**. This structure is expected to offer the proton transferring path among all three benzimidazole groups in **2** (Figure 3.7 (b)). Crystal structure analysis of **1** and sublimed **2** are in progress.

3.4.5 Effect of Temperature on Molecular Packing Structure and Hydrogen Bond network

As mentioned earlier, thermal acceleration of proton movement is important in proton transfer mechanism of PEMFC. Therefore, it is essential to study the effect of temperature on molecular arrangement of the compounds and also their hydrogen bond formations. To study the changes of packing structure affected by temperature, simultaneous WAXD-DSC measurements at temperature range from 25 to 200 °C under nitrogen atmosphere were performed. The results obtained from **1** and sublimed crystal **2** are shown in Figures 3.8 and 3.9, respectively. For compound **1**, only the peak shifts to lower degree 2θ at higher temperature and the recovery of the peak positions when the temperature decreases are observed. These changes of the peak positions imply the thermal expansion of the molecular packing structure when the temperature increased. On the other hand, the WAXD patterns of neat crystal **2** are kept unchanged in this temperature range. Moreover, the DSC thermograms of both samples show only the base-line of energy required for changing temperature without any exothermic or endothermic peaks. These results reflect that the packing structure of neat **1** and **2** molecules are stable up to 200 °C, which covers the suitable working temperature of PEMFC. For crystal **2** obtained from recrystallization, the turbid crystals, which obtained from leaving the transparent crystal in the air, were used as a sample. In contrast with **1** and **2** obtained from sublimation, the WAXD pattern of recrystallized crystal **2** is not stable in the temperature range (Figure 3.10). The peaks at 9.4 °2θ, 12.8 °2θ and 17.9 °2θ, which correspond to d-spacing of 9.39 Å, 6.89 Å and 4.97 Å, respectively, gradually

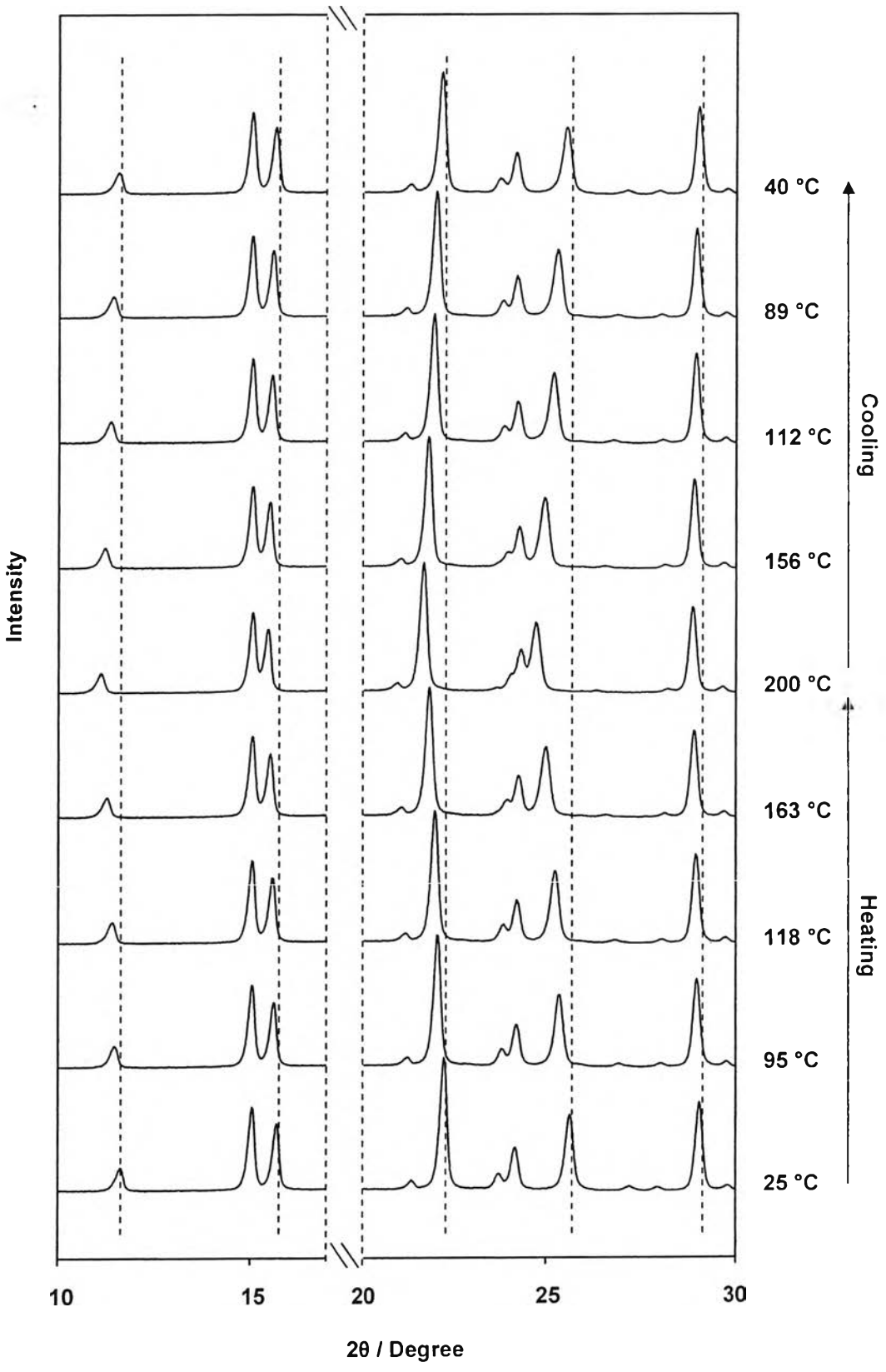

Figure 3.8 WAXD patterns of **1** at various temperatures.

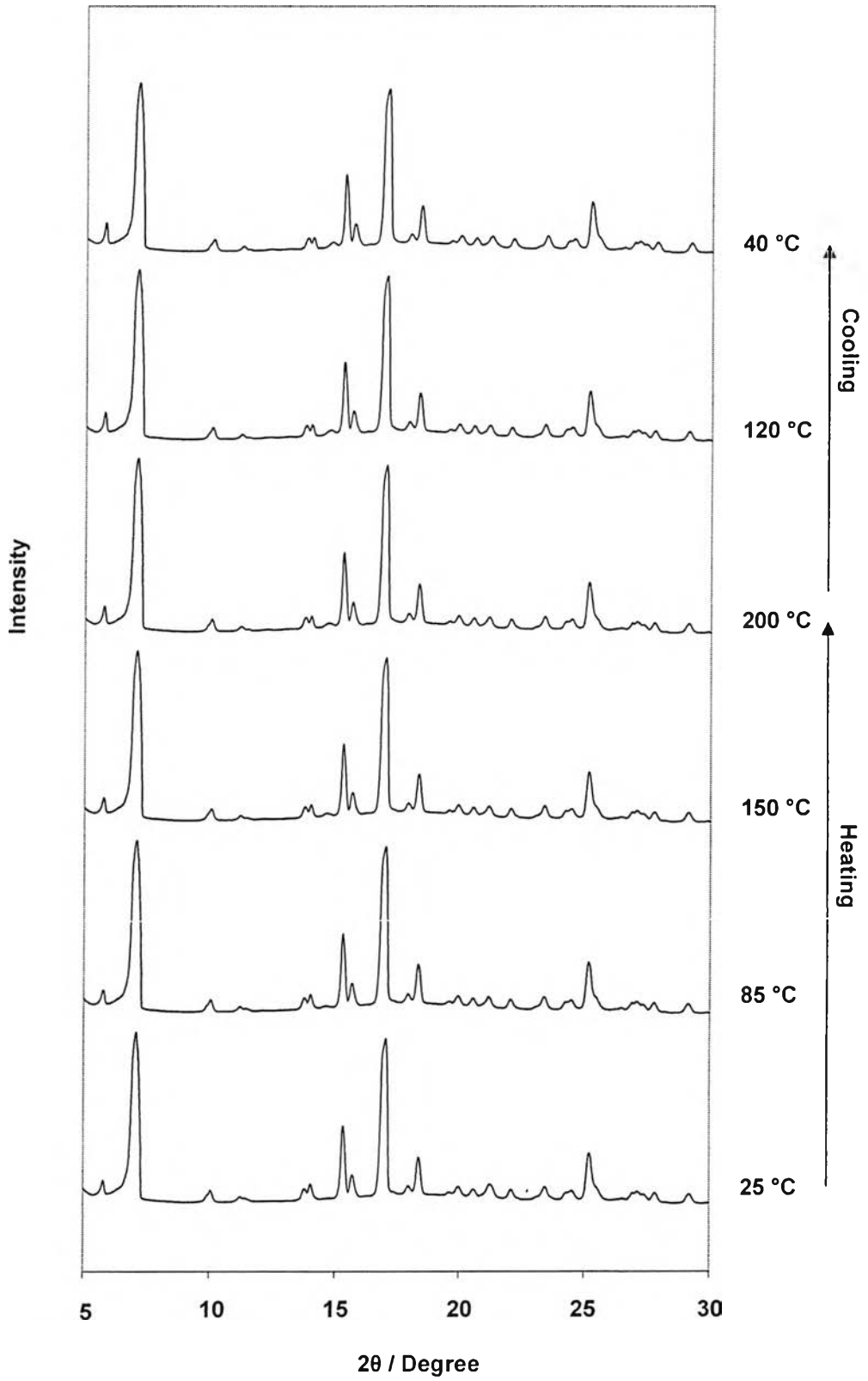

Figure 3.9 WAXD patterns of sublimed crystal **2** at various temperatures.

decrease when the sample was heated from room temperature to 75 °C (Figure 3.10 (a)). In this temperature region, the DSC thermogram shows an endothermic peak at 78 °C, corresponding to the evaporation of 2-propanol under the dry condition with nitrogen gas stream (Figure 3.10 (b)). The dry condition might accelerate solvent evaporation. At 84 °C, those two peaks completely disappeared whereas two new peaks at 15.4 °2θ and 17.1 °2θ (d-spacing 5.74 Å and 5.17 Å, respectively) are observed. At that time, the WAXD pattern of the crystal changed from recrystallized crystal **2** pattern to deformed crystal **2** pattern. This pattern is remained unchanged when the system was further heated to 150 °C and was cooled down to room temperature. The irreversible transition of the packing structure is shown around 80 °C. This transition of the packing structure might be due to the removal of solvents and caused the collapse of the molecular packing of **1** in the crystal as observed from the reduction of d-spacing from 9.39 Å, 6.89 Å and 4.97 Å to 5.74 Å and 5.17 Å. It is important to note that the peak positions and relative peak intensity of the deformed crystal **2** and sublimed crystal **2** are very similar. This hints us to speculate that molecule **2** in the crystal lattice might reorientate itself from the solvent-assisted packing structure to the non-solvent one, which is the neat crystal of **2** obtained from sublimation, after loosing solvent. However, the solid-state reorientation limits the packing of molecules and causes some disorder part in the crystal as observed from the broad peak in WAXD pattern.

Investigation of temperature effect on hydrogen bond formation was carried out by performing temperature dependent FTIR spectroscopy. The temperature-controlled sample holder was developed in our laboratory. The measurements were carried out in the temperature range of 25-250 °C. Here, FTIR spectra were collected while the samples were heating or cooling at desired temperature. Figures 3.11- 3.14 show the results obtained from benzimidazole, **1**, sublimed crystal **2**, and recrystallized crystal **2**, respectively. All samples show no significant change in fingerprint region, 1600-500 cm^{-1}. However, the important changes of the peaks in the hydrogen bond region (3600-2400 cm^{-1}) are observed. For benzimidazole, the intensity of the peaks at 3030-2500 cm^{-1} is decrease when the

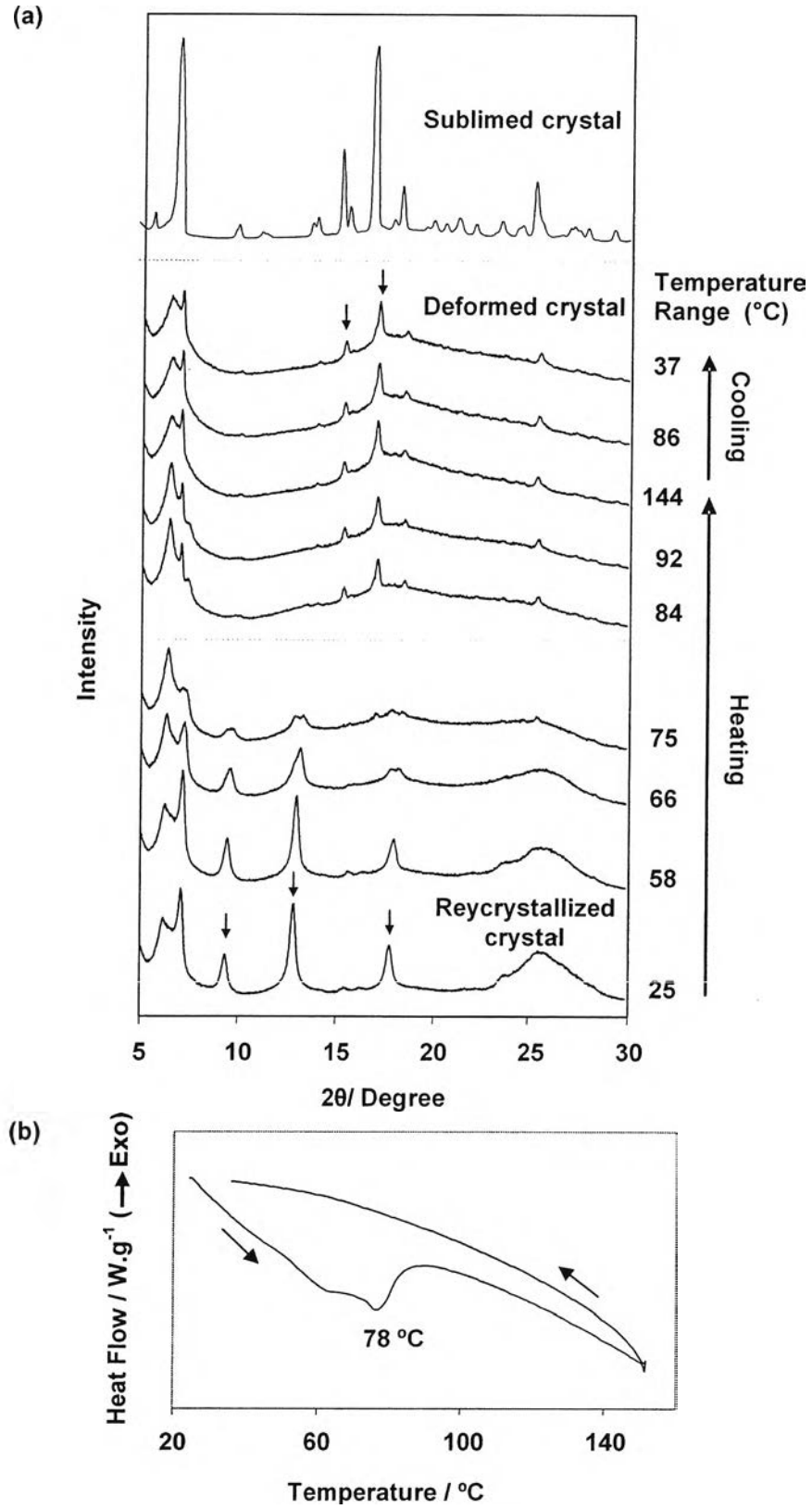

Figure 3.10 Simultaneous WAXD-DSC of **2**: WAXD patterns at various temperatures (a), and DSC thermogram (b).

sample was heated from room temperature to 160 °C. This can be explained by Scheme 3.3 (a). By heating the sample, the well-packed molecules will vibrate and move apart for some distance but still be close enough for having hydrogen bond interaction. This results in the change of the strong interaction of hydrogen bond to the weaker one and causes the decrease of the peaks intensity related to strong bonded N-H stretching, which appear in the lower frequency region (3030-2500 cm^{-1}), but increase in the intensity of the peaks correspond to weaker bonded N-H stretching, which show at higher frequency region (3100-3030 cm^{-1}). The peaks disappeared when benzimidazole was heated over its melting point (171°C). Similar to the case of benzimidazole, the bonded N-H stretching bands of **1** and **2** obtained from sublimation show the decrease of peaks intensity in low frequency region and increase of the peak intensity in high frequency region when heating the sample from room temperature to 250 °C. This change is reversible when the samples were cooled to room temperature reflecting the stability of molecular packing structure in this temperature region. The decrease in peak intensities at 3450 and 3415 cm^{-1} of **1** and sublimed crystal **2**, respectively, might be due to the change from free N-H to bonded N-H induced by thermal vibration.

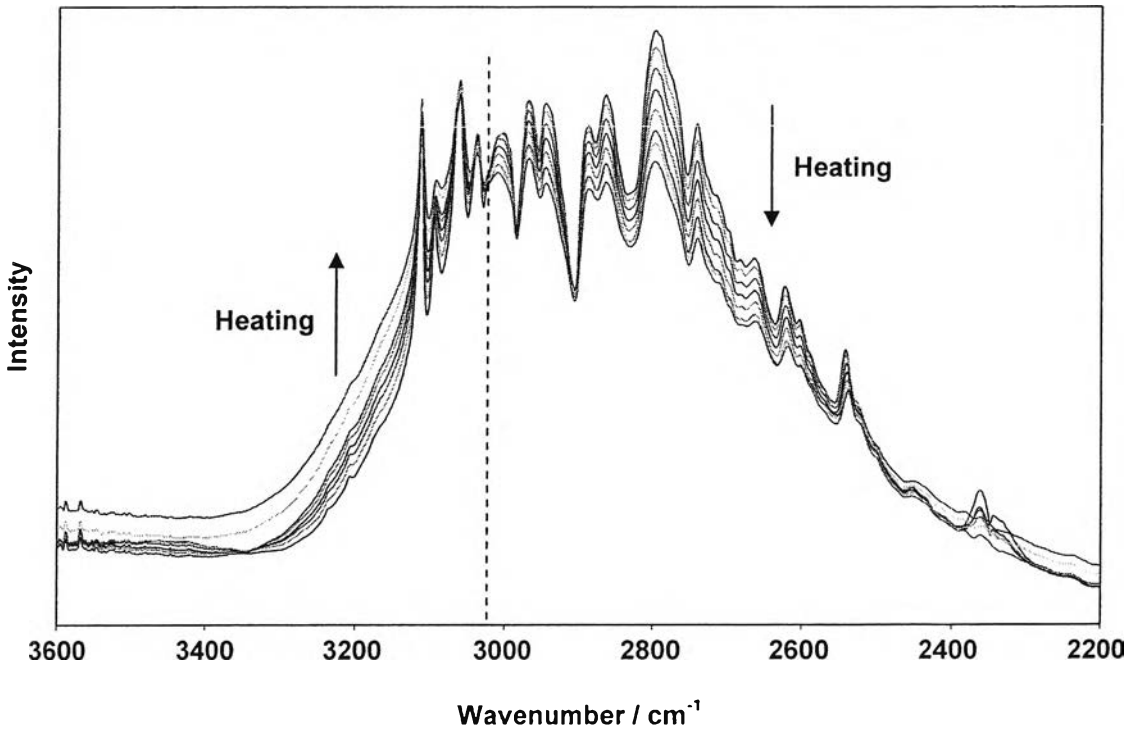

Figure 3.11 Temperature dependent FTIR spectra of benzimidazole.

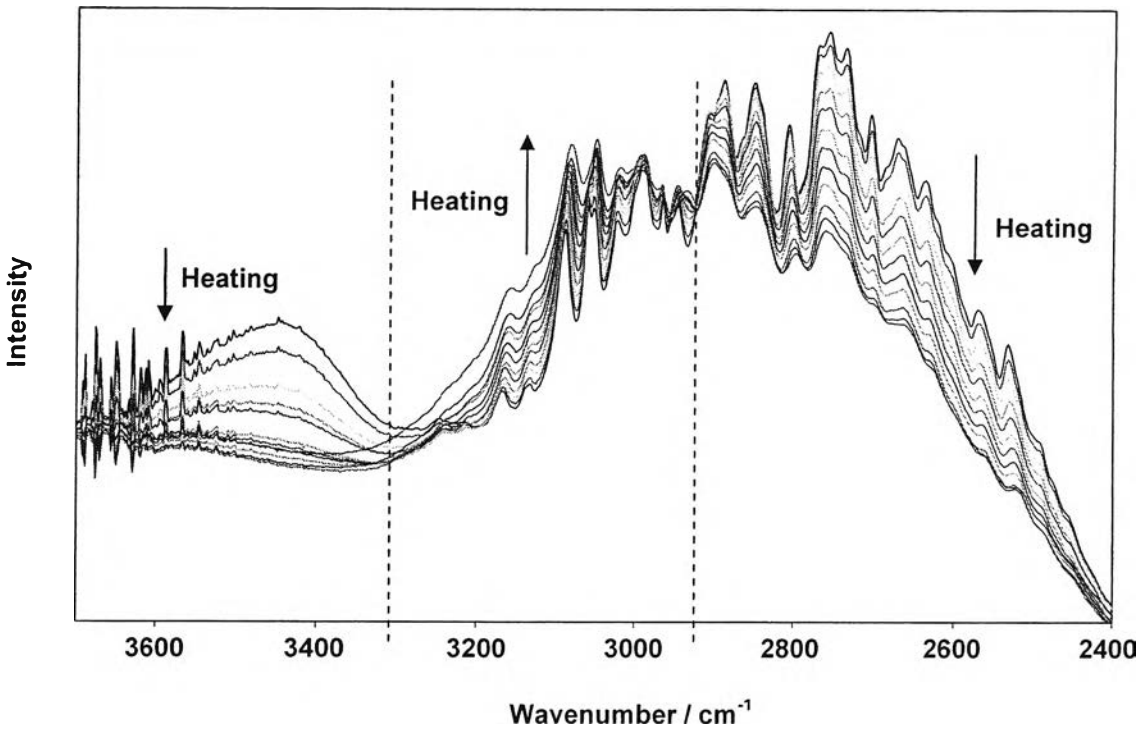

Figure 3.12 Temperature dependent FTIR spectra of **1**.

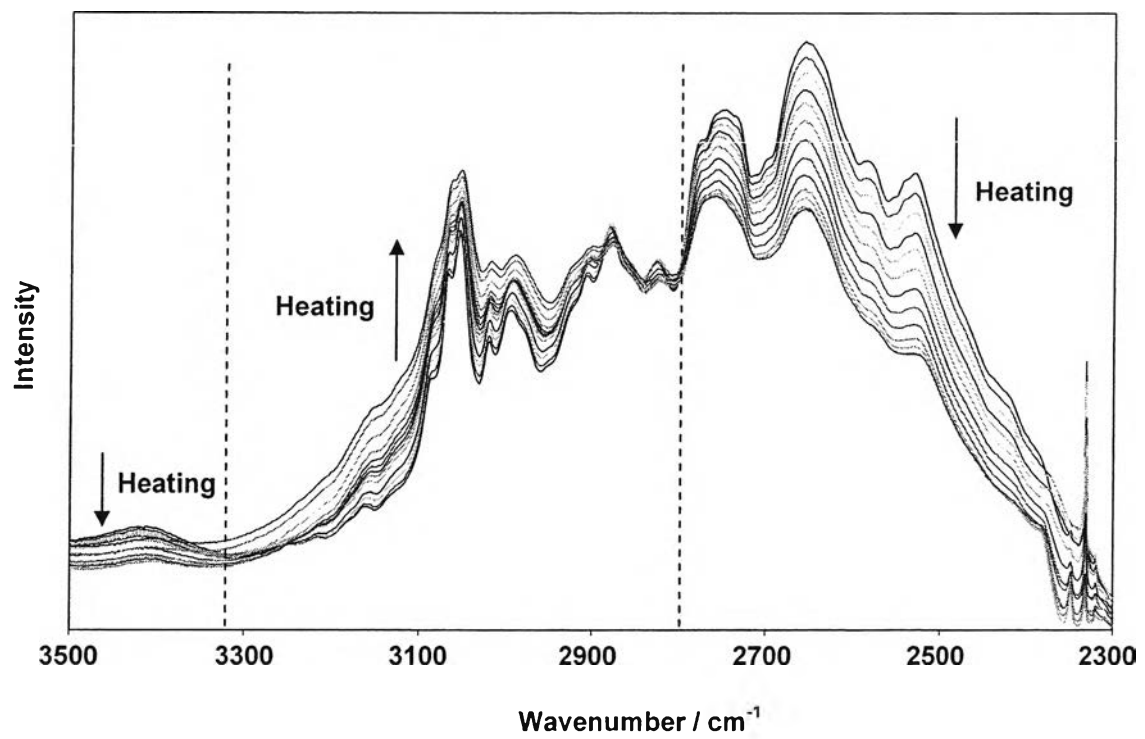

Figure 3.13 Temperature dependent FTIR spectra of sublimed crystal **2**.

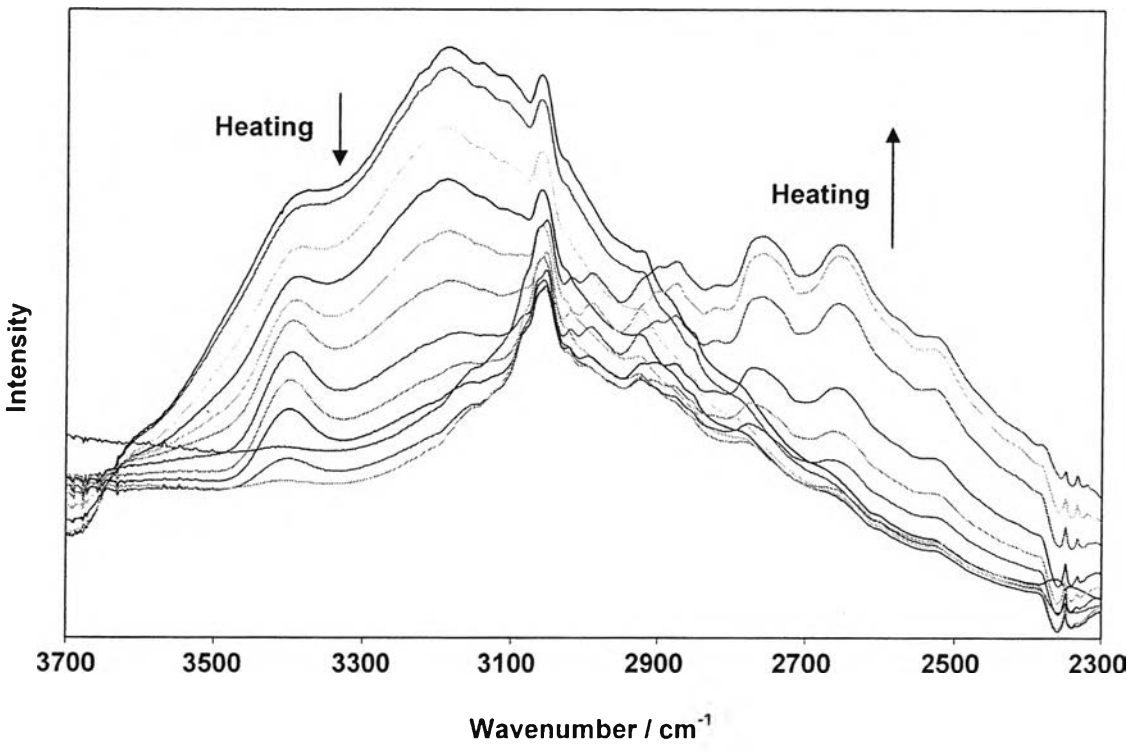

Figure 3.14 Temperature dependent FTIR spectra of crystal **2** obtained from solution-recrystallization.

It should be noted that when compare the positions that peak intensities of bonded N-H stretching change from decrease to increase under higher temperature between benzimidazole, **1** and **2** obtained from sublimation, which are 3030, 2930 and 2810 cm^{-1}, respectively, it might be reasonable to speculate that the strength of hydrogen bond interactions are in order of **2** > **1** > benzimidazole as **2** can retain the change of stronger bonded N-H stretching peaks than **1** whereas benzimidazole is the weakest. This can be explained by the fact that molecule **2** is a stiff, bulky and planar shape structure which makes it be difficult to form side-by-side hydrogen bond as observed in the case of benzimidazole. Therefore, the molecular packing should be derived by the stacking conformation as seen in Scheme 3.3 (b) and results in the strong interaction between molecules governed by both hydrogen bond and π-π interaction. This reflects to the more difficult of molecular movement under high temperature. In case of recrystallized **2**, we can clearly observe the change of the hydrogen bond pattern from O-H type to N-H type when the sample was heated from room temperature to 250 °C.

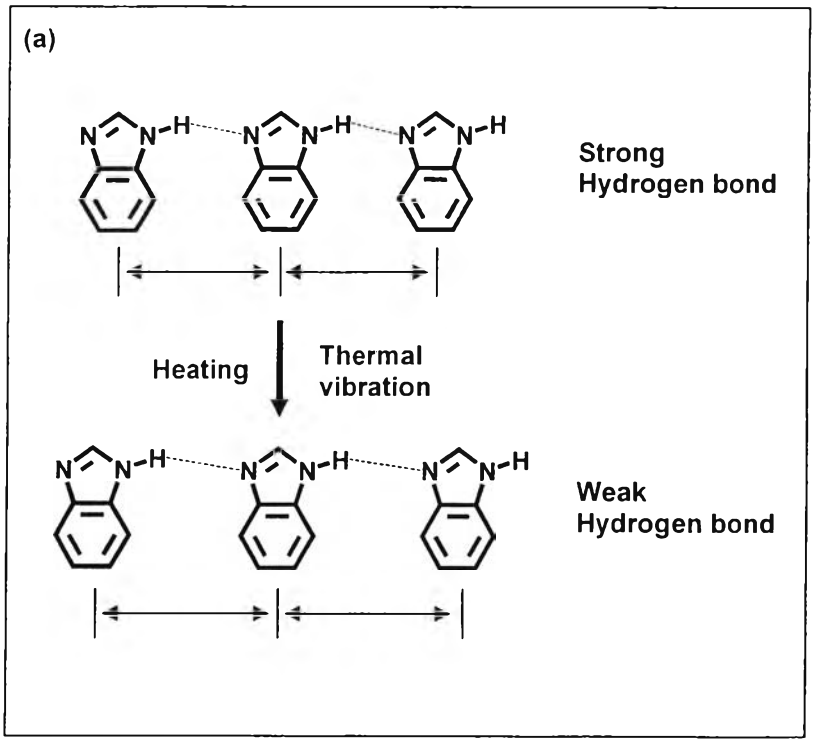

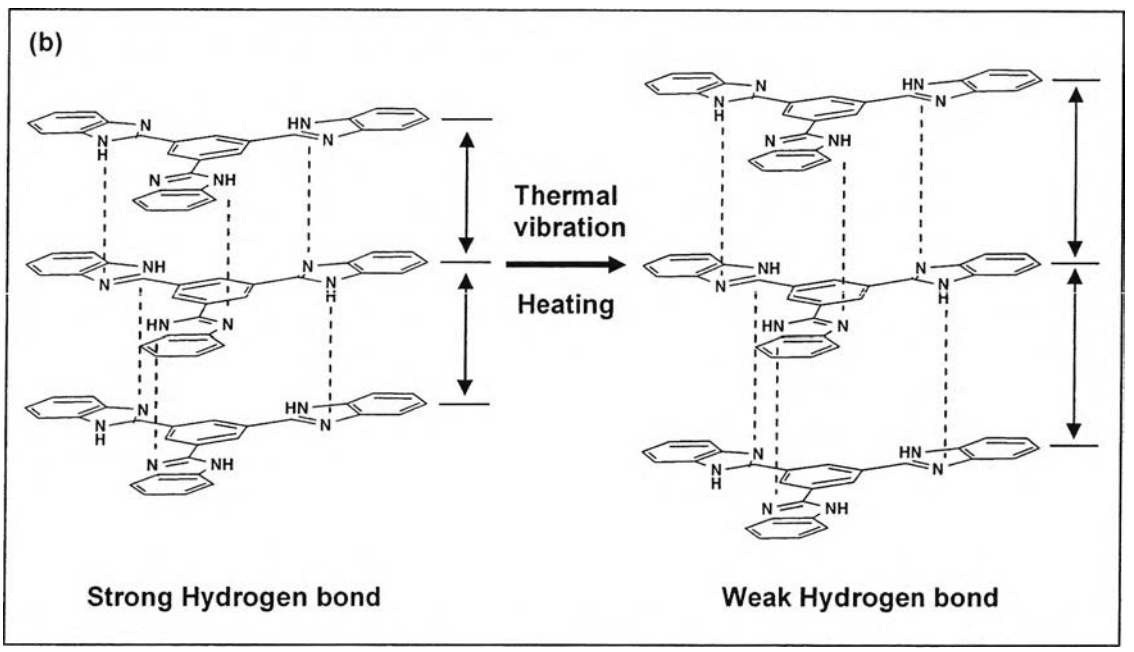

Scheme 3.3 Increment of intermolecular distance induced by increasing temperature: benzimidazole (a), and **2** (b).

This also confirm the evaporation of 2-propanol from crystal lattice at high temperature. Based on the studies of molecular packing structure, hydrogen

bond formation, crystal structure analysis and the temperature effects of **1** and **2** in comparison with those of benzimidazole, we expect that our strategy to enhance the packing of benzimidazole unit by either increase the number of benzimidazole group in the molecule or induce π-π stacking conformation via planar shape structure will make our model compounds being the useful structures for developing effective proton hopping path. Measuring of their proton conductivities are in progress.

3.5 Conclusion

Di- and trifunctional benzimidazole compounds, **1** and **2**, were designed and successfully synthesized by the reaction between acid chloride and diamine. The Compounds showed highly thermally stable property over 400 °C. Characterizations revealed the possibly well-packed structure with intermolecular hydrogen bond network similar to the one observed in benzimidazole. For compound **2**, X-ray structure analysis illustrated the molecular complex between one molecule of **1** and six molecule of 2-propanol resulting in the solvent-assisted intramolecular hydrogen bonds network. The neat packing structure of **1** and **2** showed higher thermal stability than that of benzimidazole implying the stronger molecular interaction than single benzimidazole unit. The works clarified a possibility of di- and trifunctional benzimidazole with hydrogen bond network which may favor the proton movement at high operating temperature required for PEMFC.

3.6 Supporting Information

Crystallographic data (excluding structure factors) for the structures in this paper have been deposited with the Cambridge Crystallographic Data Centre as supplementary publication numbers CCDC 671942 (**1**) and CCDC 675661 (benzimidazole). Copy of the data can be obtained, free of charge, on application to CCDC, 12 Union Road, Cambridge CB2 1EZ, UK, (fax: +44-1223-336033 or e-mail: deposit@ccdc.cam.ac.uk).

3.7 Acknowledgment

The authors acknowledges the Thailand Government Research Budget (National Research Council of Thailand), the NRCT-JSPS joint research program (National Research Council of Thailand and Japan Society for Promotion of Science), the Engineering Research and Development Project (National Metal and Materials Technology Center of Thailand), and Research Task Force (Chulalongkorn University) for their supports. The appreciation is also to Dr. Suttinun Phongthamrug for crystal analysis.The work was mainly done under the Royal Golden Jubilee Ph.D. Scholarship (grant no. PHD/0031/2547) (the Thailand Research Fund).

3.8 References

[1] M. Watanabe, H. Igarashi, H. Uchida, F. Hirasawa, *J. Electroanal. Chem.* **1995,** *399*, 239.

[2] K. D. Kreuer, *J. Membr. Sci.* **2001**, *185*, 29.

[3] G. Alberti, M. Casciola, *Solid State Ionics* **2001**, *145*, 3.

[4] K. D. Kreuer, *Solid State Ionics* **1997**, *94*, 55.

[5] K. D. Kreuer, *Solid State Ionics* **2000**, *136-137*, 149.

[6] C. Yang, P. Costamagna, S. Srinivasan, J. Benziger, A. B. Bocarsly, *J. Power Sources* **2001**, *103*, 1.

[7] J. C. Persson, P. Jannasch, *Chem. Mater.* **2003**, *15*, 3044-3045.

[8] O. Savadogo, *J. Power Sources* **2004**, *127*, 135.

[9] J. Divisek, H. F. Oetjen, V. Peinecke, V. M. Schmidt, U. Stimming, *Electrochim. Acta* **1998**, *43*, 3811.

[10] U. Beuscher, S. J. C. Cleghorn, W. B. Johnson, *Int. J. Energy. Res.* **2005**, *29*, 1103.

[11] D. J. Jones, J. Rozière, *J. Membr. Sci.* **2001**, *185*, 41.

[12] K. D. Kreuer, A. Fuchs, M. Ise, M. Spaeth, J. Maier, *Electrochim. Acta* **1998**, *43 (10-11)*, 1281.

[13] M. Yamada, I. Honma, *Electrochim. Acta* **2003**, *48*, 2411.

[14] M. F. H. Schuster, W. H. Meyer, M. Schuster, K. D. Kreuer, *Chem. Mater.* **2004**, *16*, 329.

[15] M. Münch, K. D. Kreuer, W. Silvestri, J. Maier, G. Seifert, *Solid State Ionics* **2001**, *145*, 437.

[16] J. A. Asensio, P. Gómez-Romero, *Fuel Cells* **2005**, *5 (3)*, 336.

[17] A. Carollo, E. Quartarone, C. Tomasi, P. Mustarelli, F. Belotti, A. Magistris, F. Maestroni, M. Parachini, L. Garlaschelli, P. P. Righetti, *J. Power Sources* **2006**, *160*, 175.

[18] A. Bozkurt, W. H. Meyer, *Solid State Ionics* **2001**, *138*, 259.

[19] J. C. Persson, K. Josefsson, P. Jannasch, *Polymer* **2006**, *47*, 991.

[20] Y. Fu, A. Manthiram, D. G. Michael, *Electrochem. Commun.* **2007**, *9*, 905.

[21] M. Yamada, I. Honma, *Polymer* **2005**, *46*, 2986.

[22] J Sun, L. R. Jordan, M. Forsyth, D. R. MacFarlane, *Electrochim. Acta* **2001**, *46*, 1703.

[23] Y. F. Liu, Q. C. Yu, Y. H. Wu, *Electrochim. Acta* **2007**, *52*, 8133.

[24] S. Phongtamrug, K. Tashiro, M. Miyata, S. Chirachanchai, *J. Phys. Chem. B.* **2006**, *110*, 21365.

[25] N. Vijayan, N. Balamurugun, R. Ramesh Babu, R. Gopalakrishnan, P. Ramasmy, W. T. A. Harrison, *Journal of Crystal Growth.* **2004**, *267*, 218.

[26] N. Vijayan, G. Bhagavannarayana, T. Kanagasekaran, R. Ramesh Babu, R. Gopalakrishnan, P. Ramasmy, *Cryst. Res. Technol.* **2006**, *41*, 284.

Additional Information

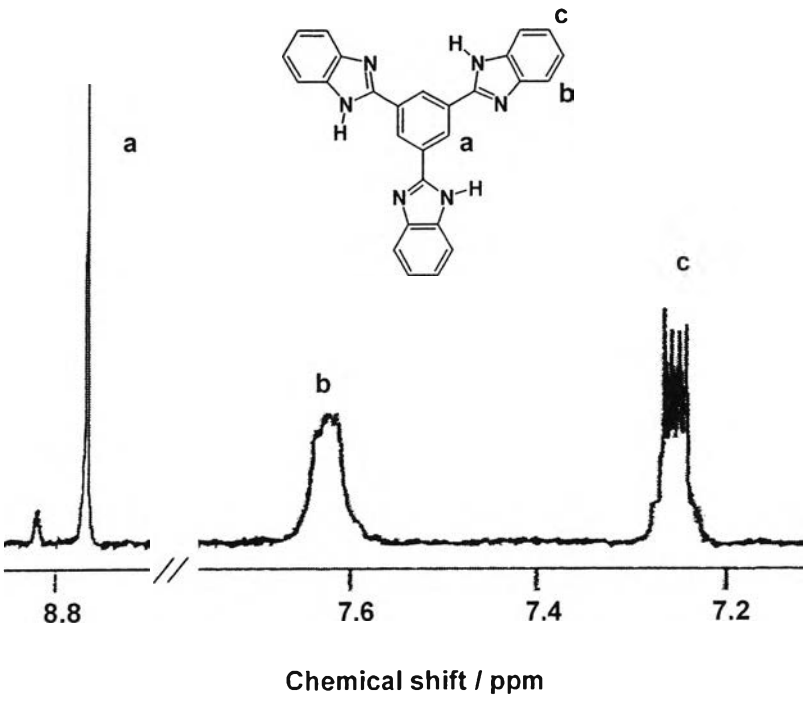

NMR spectrum of **2**.

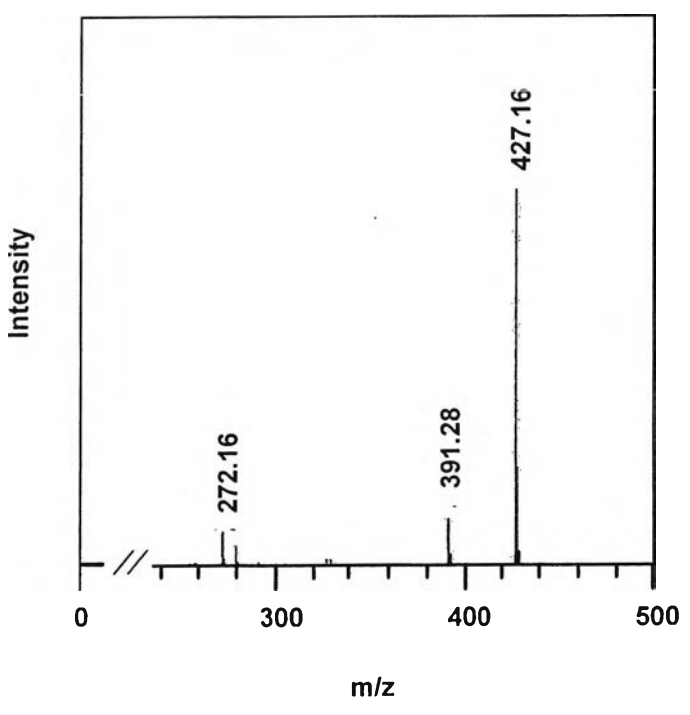

Mass spectrum of **2**.